

Laser Photofragment Spectroscopy of Near-Threshold Resonances in SiH⁺ [and Discussion]

P. J. Sarre, J. M. Walmsley, C. J. Whitham and G. Duxbury

Phil. Trans. R. Soc. Lond. A 1988 **324**, 233-246

doi: 10.1098/rsta.1988.0014

Email alerting service

Receive free email alerts when new articles cite this article - sign up in the box at the top right-hand corner of the article or click [here](#)

To subscribe to *Phil. Trans. R. Soc. Lond. A* go to: <http://rsta.royalsocietypublishing.org/subscriptions>

Laser photofragment spectroscopy of near-threshold resonances in SiH^+

BY P. J. SARRE, J. M. WALMSLEY AND C. J. WHITHAM

*Department of Chemistry, University of Nottingham, University Park,
Nottingham NG7 2RD, U.K.*

Near-threshold resonances in the photodissociation cross section of SiH^+ have been recorded by the detection of photofragment Si^+ ions. The photodissociation spectrum is found to be dominated by Feshbach resonances. The first evidence for multichannel resonances in the photodissociation spectrum of a diatomic molecule is presented.

Laser photodissociation spectra between $15\,600\text{ cm}^{-1}$ and $18\,750\text{ cm}^{-1}$ were recorded at a resolution of 0.0012 cm^{-1} by coaxial laser irradiation of a fast ion beam of SiH^+ . Over 70 transitions were observed, the majority of which involve excited-state levels (resonances) that lie between the $\text{Si}^+(^2\text{P}_{3/2}) + \text{H}(^2\text{S})$ and $\text{Si}^+(^2\text{P}_{1/2}) + \text{H}(^2\text{S})$ dissociation limits, which are separated by 287 cm^{-1} . The assignments were made by combining experimental information with predictions of the vibrational and rotational energy levels obtained by numerical solution of the radial Schrödinger equation and calculations of the rotational line intensities. The experimental data were obtained by measurement of the transition frequencies, line intensities, linewidths and hyperfine splittings and through examination of the effect of laser power on the linewidth. The kinetic energy released on dissociation and the photofragment angular distribution were also determined.

INTRODUCTION

The rovibronic energy levels of well-separated electronic states in a diatomic molecule near to its equilibrium internuclear configuration are usually well described within the Born–Oppenheimer approximation. By using spectroscopic data or the results of *ab initio* calculations, it is possible to obtain potential-energy surfaces that describe the vibrational and rotational motion of the nuclei in this region. At the other extreme, the electronic structures of the isolated atomic fragments can usually be established by electronic spectroscopy and at least an approximate long-range potential between the atoms may be calculated. The last few vibrational levels of a molecule just below dissociation have a different character from those near the bottom of the well (Stwalley 1978), and in the absence of non-adiabatic effects their energies and wavefunctions are almost totally determined by the long-range form of the interatomic potential (Stwalley 1978; LeRoy & Bernstein 1970). The region of intermediate internuclear separation is difficult to probe experimentally and only in a very few cases has the structure of a molecule been investigated up to its dissociation limit.

The near-dissociation behaviour of a diatomic molecule is of particular interest when one or both of the atomic fragments possess electronic angular momentum. It then follows that more than one molecular electronic state must correlate to the same dissociation limit. For example, the four lowest-lying electronic states of the SiH^+ molecular ion all correlate with the $\text{Si}^+(^2\text{P}) + \text{H}(^2\text{S})$ dissociation asymptote as shown in figure 1. In the near-dissociation region, the energy separation of the electronic states becomes comparable to the magnitude of non-

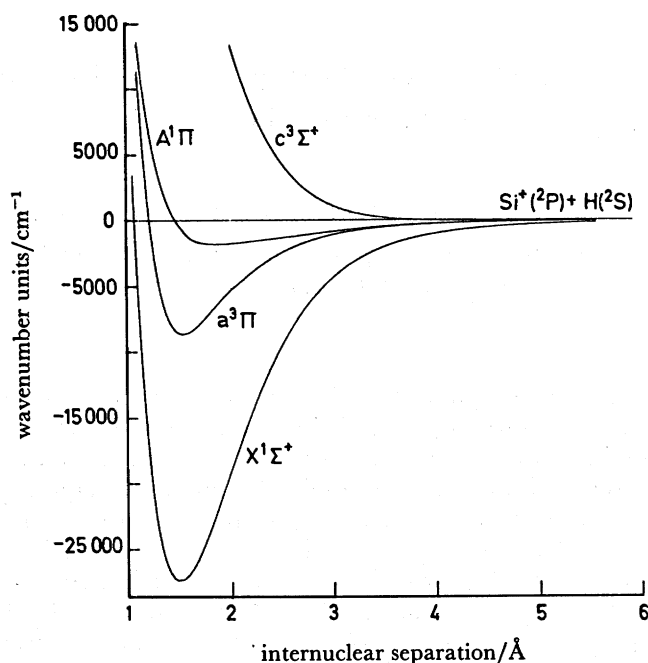


FIGURE 1. Composite experimental-theoretical potential-energy curves for SiH^+ excluding spin-orbit coupling. The derivation of the singlet curves is described in the text. The $^3\Pi$ and $^3\Sigma^+$ curves are from Hirst (1986) with the $^3\Pi$ well located in accordance with the results of Berkowitz *et al.* (1987).

adiabatic interactions between the Born-Oppenheimer states. Accordingly, it is anticipated that spin-orbit and Coriolis coupling may no longer be treated as a small perturbation within a Born-Oppenheimer basis. The effect of non-adiabatic interactions is expected to be revealed through their influence on the positions of the energy levels just below and also just above the dissociation threshold and also on the character of their corresponding wavefunctions. The molecular fragmentation dynamics will also be very sensitive to these interactions. Levels above dissociation are also quite properly described as scattering resonances. The nature of near-threshold resonances when non-adiabatic interactions are important has recently been examined in a series of theoretical papers by Freed & co-workers, who have predicted the existence of many interesting novel effects in the photofragmentation spectra of diatomic molecules that dissociate into open-shell atoms (Singer *et al.* 1985; Williams & Freed 1986; Williams *et al.* 1987).

In principle, a wealth of information on the intermediate (recoupling) region may be obtained from spectroscopic experiments on energy levels just below threshold. In practice, it is probably easier to obtain spectra involving energy levels just above dissociation by recording photofragment spectra. The spectroscopic experiment allows detection of much narrower resonances than is possible in atomic scattering experiments that are subject to relatively poor translational-energy resolution and no control over the impact parameter. One experimental approach to the study of near-threshold resonances is via the laser photodissociation of molecular ions in fast ion beams (for a review, see Moseley 1985), and in this paper we describe experiments of this type on the SiH^+ ion. Feshbach resonances are found to be dominant and the first evidence for multichannel resonances in the photodissociation spectrum of a diatomic molecule is described.

NEAR-THRESHOLD RESONANCES IN THE DISSOCIATION OF DIATOMIC MOLECULES

Resonances (or metastable levels) that lie just above the dissociation threshold can be considered to arise in two ways. Firstly, levels may be trapped behind a 'hump' or barrier in the potential. A barrier can arise from the contribution of a centrifugal term to the effective potential because of rotation of the molecule, although a 'hump' may already exist in the potential of the non-rotating molecule because of an avoided crossing between states of the same symmetry. Secondly, Feshbach resonances occur where bound levels that belong to one potential curve lie embedded in the continua of one or more electronic states that correlate to a lower dissociation asymptote. We include in the following discussion those resonances that only occur in the near-threshold dissociation region (for a more general discussion see Lefebvre-Brion & Field 1986).

Shape resonances, which can also be described as centrifugally bound levels, arise from the introduction of a centrifugal barrier in the effective potential of a rotating diatomic molecule. The centrifugal energy term is added to the potential of the non-rotating molecule $U_0(R)$ to yield an effective potential, $U_{\text{eff}}(R)$, which may be written

$$U_{\text{eff}}(R) = U_0(R) + (\hbar^2/2\mu R^2) [J(J+1) - \Omega^2].$$

Solution of the Schrödinger equation for the nuclei with this potential yields eigenenergies that lie below and also above the dissociation asymptote of $U_0(R)$. Those levels that are above the dissociation limit are termed shape resonances and have associated predissociation lifetimes that are determined by the probability of tunnelling through the centrifugal barrier. In scattering terminology such quasibound levels are 'single channel' resonances, as only one potential energy surface is involved. Examples of shape resonances in molecular ions recently observed by fast-ion-beam laser photofragment spectroscopy include studies of HeH^+ (Carrington *et al.* 1981, 1983) and CH^+ (Helm *et al.* 1982; Carrington & Softley 1986; Sarre *et al.* 1986, 1987). The situation is in fact more complex in a molecule such as CH^+ or SiH^+ because shape resonance levels of one state lie in the continua of other electronic states that correlate to the same dissociation limit. With reference to figure 1, it can be seen that a rotationally quasibound level of the $^1\Pi$ state in SiH^+ would be susceptible to predissociation by coupling to the continua of the $^1\Sigma^+$ and $^3\Pi$ states. The influence of these states has been identified in the linewidths recorded in the corresponding photopredissociation spectra of the isovalent molecule CH^+ (Graff *et al.* 1983; Sarre *et al.* 1986, 1987). The language employed here assumes that the level structure and predissociation rates can be treated satisfactorily within a Born–Oppenheimer basis. In broad terms this appears to be the case for the high-lying quasibound levels of CH^+ that have been studied to date. A good example of the case where there is already a 'hump' in the potential is found in the absorption ($A^1\Pi - X^1\Sigma^+$) spectrum of the AlH molecule (which is isoelectronic with SiH^+). The $^1\Pi$ curve has a potential 'hump' (Herzberg & Mundie 1940) with a height of *ca.* 0.15 eV (Hurley 1961) and it is found that the higher rotational levels of $v' = 0$ and 1 are trapped behind the barrier but lie above the dissociation limit (Herzberg 1950). For the SiH^+ molecule, *ab initio* calculations show no evidence for a 'hump' in the potential of the $^1\Pi$ state (Hirst 1986, 1987) so this aspect is not of direct importance here.

Secondly, Feshbach resonances occur when an energy level that is nominally derived from one potential energy surface and that is located below the dissociation asymptote to which that

surface correlates, lies above a lower dissociation limit or channel. An example is provided in the work reported here and is illustrated in figure 2. The ${}^1\Pi_1$ state correlates to the upper $\text{Si}^+({}^2P_{3/2}) + \text{H}({}^2S)$ fine-structure dissociation limit and so a number of levels of this state lie between the fine-structure dissociation asymptotes. The photodissociation spectra of SiH^+

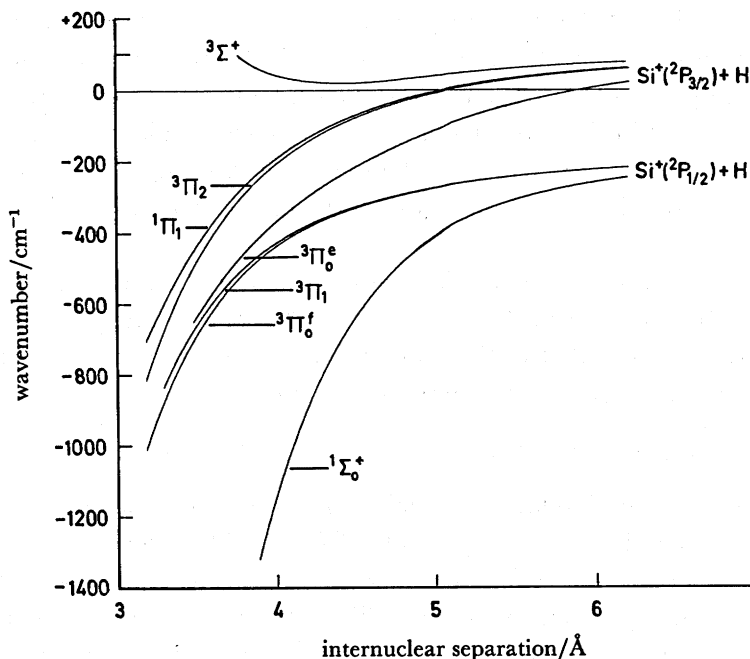


FIGURE 2. Correlation of molecular and atomic states for $J = 2$ including spin-orbit coupling. For simplicity, only seven of the twelve potentials are shown. The spin-orbit splitting in the Si^+ ion is 287 cm^{-1} .

recorded in this study arise predominantly from transitions to levels between the two dissociation limits. Predissociation occurs by coupling of the ${}^1\Pi$ levels to states that correlate to the lower asymptote, i.e. $\text{SiH}^+({}^2P_{1/2}) + \text{H}({}^2S)$, which lies 287 cm^{-1} below the $\text{Si}^+({}^2P_{3/2}) + \text{H}({}^2S)$ limit. A similar case was found in the infrared predissociation spectrum of HeNe^+ (Carrington & Softley 1985).

In reality, this outline of near-threshold resonances is an oversimplification of the problem for SiH^+ . Our results show evidence of strong mixing of Born–Oppenheimer states through spin-orbit and Coriolis interactions, which have a profound effect on the spectrum. The simplest photodissociation spectrum of SiH^+ that could be obtained would arise from excitation from the $X^1\Sigma^+$ state to predissociated levels of the $A^1\Pi$ state for which the selection rules are $\Delta J = 0$ (Q) and $\Delta J = \pm 1$ (R, P). The excited-state levels could be either of the shape resonance or Feshbach type. Non-adiabatic couplings tend to weaken this ‘isolated state’ model in the near-dissociation region and consequently additional lines may be found in the spectra. This is in accord with theoretical predictions of the photodissociation cross sections based on the results of fully coupled multichannel calculations of the resonances (Williams *et al.* 1986, 1987). The extra lines involve upper-state levels that are derived from potentials other than the ${}^1\Pi$ state and that correlate to the $\text{Si}^+({}^2P) + \text{H}({}^2S)$ asymptotes. When substantial mixing involving two or more different states occurs, it is appropriate to call the resultant resonances (levels) ‘multichannel’ in character. For the CH^+ molecule, it has been predicted that multichannel

resonances would be found on photoexcitation from the ground electronic state (Williams *et al.* 1986, 1987), but to date no firm experimental evidence for such resonances has been reported. In fact, an alternative and completely different assignment has been proposed for the known additional lines that occur in the CH^+ photodissociation spectrum near 540 nm (Helm *et al.* 1982; Sarre *et al.* 1986, 1987) and also near 350 nm (Cosby *et al.* 1980; Sarre & Whitham 1987). Complex spectra in the infrared predissociation spectrum of CH^+ have been reported (Carrington & Softley 1986), but the authors did not find any evidence for multichannel resonances. In this paper we describe the observation of multichannel resonances in the photodissociation of SiH^+ . To the best of our knowledge this is the first identification of such resonances in the photodissociation spectrum of any molecule.

EXPERIMENTAL CONSIDERATIONS

Laser photofragment spectra are recorded by irradiation of a mass-selected ion beam with tunable laser radiation and detection of the photoproduct ions. The apparatus is illustrated in figure 3. A 10^{-7} A beam of SiH^+ ions is generated by 70 eV electron-impact ionization of silane

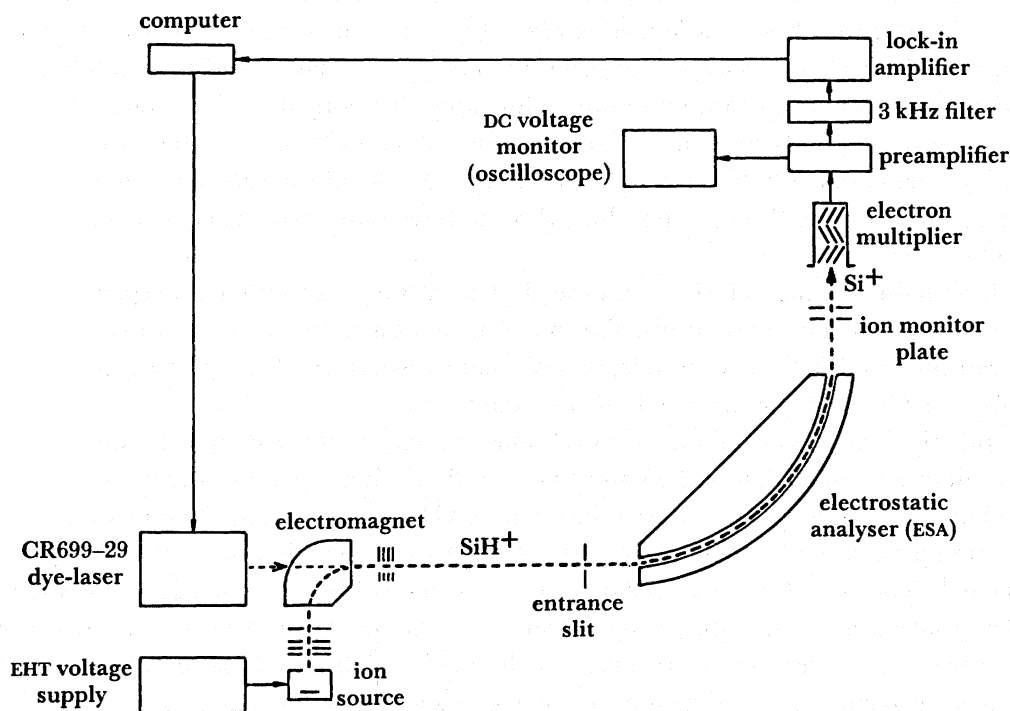


FIGURE 3. Schematic diagram of the fast-ion-beam apparatus. Photofragmentation of SiH^+ to form Si^+ is shown.

in a conventional mass-spectrometric ion source and is accelerated to an energy of 3.7 keV. A small 6 cm radius electromagnet provides mass separation of the SiH^+ ions from the other ions created in the ionization process. Tunable radiation from a Coherent CR-590 (broadband) or CR-699-29 Autoscan (single mode) dye laser is merged coaxially with the ion beam over a path length of 0.5 m and induces transitions from levels of the ground electronic state to near-threshold predissociated levels. Provided that the lifetime of the level towards dissociative decay is sufficiently short, the parent ion dissociates in the flight region into Si^+ and H fragment

atoms. An electrostatic energy analyser (ESA) is used to separate the Si^+ ions from the parent beam and these are then detected with an electron multiplier. The ESA also serves to measure the translational energy released in the fragmentation process.

When the single-mode laser is employed, the spectroscopic resolution is determined by the energy spread in the SiH^+ beam. This is typically 0.5 eV (FWHM) and, because of the effect of kinematic compression in an accelerated beam (Kaufman 1976), this corresponds to a Doppler width of only 35 MHz at a laser wavenumber of $17\,500\text{ cm}^{-1}$. This narrow linewidth is of considerable value as it is sufficient to permit the resolution of proton nuclear hyperfine splittings in many instances. In other cases, where the predissociation lifetime of the level is sufficiently short, the effect of lifetime broadening outside the Doppler width can be observed. Hyperfine splitting and lifetime broadening are generally mutually exclusive features in the spectra. The laser delivers a power of up to 950 mW and this is sufficient to saturate many of the transitions and induce power broadening. Consequently the power has to be reduced for some of the measurements. Transitions to levels with triplet character have a smaller oscillator strength and in most cases do not exhibit line broadening at high laser power. This is also useful in assigning the spectrum.

The ESA permits measurement of the kinetic-energy release associated with laser excitation to a specific level that has well-defined energy, angular momentum and parity. In this work, the centre-of-mass energy release is at most 50 meV (*ca.* 400 cm^{-1}) but fortunately the transformation to the laboratory frame results in an 'amplification' in which a 50 meV centre-of-mass release corresponds to a much larger spread of 17.4 eV in the laboratory frame for a parent-ion energy of 3.7 keV. To obtain the energy release information a deconvolution of the peak shape is desirable. We have not done this but have estimated the energy release from the FWHM of the recording.

The laser light is plane polarized and the electric vector necessarily lies perpendicular to the ion-beam direction. The angular distribution of the photoproduct ions is sensitive to the nature of the transition and so the energy-release peak shape reveals whether a given spectroscopic line arises from $\Delta J = 0$ (Q) or $\Delta J = \pm 1$ (R, P) excitation.

The principal source of noise is from Si^+ ions, which are formed by collision-induced and unimolecular decomposition of the parent beam. Discrimination against these ions is achieved by mechanical chopping of the laser beam at 3 kHz and by using lock-in detection. The lasers were operated with Rhodamine-110, -6G and -B dyes, which covered the range $18\,750\text{--}15\,600\text{ cm}^{-1}$. The broad-band CR-590 laser has a linewidth of *ca.* 20 GHz and was used to record a rapid survey scan of the strongest features of the spectrum. All of the spectroscopic and energy-release measurements were made with the CR-699-29 Autoscan system, which incorporates a wavemeter and gives a measurement accuracy better than $\pm 0.005\text{ cm}^{-1}$. The use of a fast beam introduces a Doppler shift of about $8\text{--}10\text{ cm}^{-1}$ depending on the wavelength. The ion-beam energy and precise Doppler shifts were determined by measuring the frequency of a strong narrow spectroscopic line with both parallel and antiparallel coaxial irradiation of the laser and ion beams.

SPECTROSCOPY AND POTENTIAL-ENERGY CURVES OF SiH^+

The first spectroscopic data on SiH^+ were obtained by Douglas & Lutz (1970), who recorded the 0-0, 0-1, 0-2, 1-0 and 1-1 bands of the $\text{A}^1\Pi\text{--X}^1\Sigma^+$ system in emission from a hollow-cathode discharge containing helium with a trace of silane. This led to the definitive identi-

fication of SiH^+ in the solar photosphere (Grevesse & Sauval 1970). The $^1\Pi$ state was found to have a very shallow well with a $\Delta G_{\frac{1}{2}}$ value of only 390.17 cm^{-1} . In subsequent work (Carlson *et al.* 1980), two additional bands (2–0 and 3–0) were recorded and analysed and the lifetimes for $v' = 0, 1, 2$ and 3 were measured. The observation of transitions involving $v' = 2$ and 3 led to a revision of the dissociation energy of the $^1\Pi$ state and a value for $D_0(^1\Pi)$ of $1230 \pm 210 \text{ cm}^{-1}$ ($0.15 \pm 0.03 \text{ eV}$) was deduced.

A photoionization mass-spectrometric study of the SiH radical has provided new information including a measurement of the ionisation potential of SiH (Berkowitz *et al.* 1987). A number of autoionization features were observed, some of which were attributed to a Rydberg series converging to the $a^3\Pi$ state of SiH^+ . This is the first experimental information on the location of this triplet state with respect to the singlet-state manifold. The difference in energy between the $X^1\Sigma^+$ and $a^3\Pi$ states was deduced to be $2.30 \pm 0.01 \text{ eV}$, which is in reasonable agreement with the results of two *ab initio* calculations (Bruna *et al.* 1983; Hirst 1986).

Ab initio calculations of the SiH^+ potential-energy curves have been reported by Bruna & Peyerimhoff (1983), Bruna *et al.* (1983) and Hirst (1986), although the first two publications did not contain the numerical data. Hirst (1986) calculated the surfaces for the $X^1\Sigma^+$, $A^1\Pi$, $a^3\Pi$ and $c^3\Sigma^+$ states by using the multireference *ci* method and showed that there was no evidence for a maximum in the $^1\Pi$ state.

RESULTS AND ASSIGNMENTS

This work was initiated to provide a complementary study to the photodissociation spectrum of CH^+ in which numerous shape resonances have been identified (Helm *et al.* 1982; Sarre *et al.* 1986, 1987a). In SiH^+ , the $A^1\Pi$ state is substantially shallower than the corresponding state in CH^+ for which $D_0(^1\Pi)$ is 1.159 eV (Helm *et al.* 1982; Graff *et al.* 1983). In contrast to CH^+ , we have found that the photodissociation spectrum is dominated by Feshbach resonances. A significant difference between the two cases is the larger spin-orbit splitting of 287 cm^{-1} in Si^+ compared with 63 cm^{-1} in C^+ . In figure 2 it is shown that the $A^1\Pi$ state correlates to the upper fine-structure limit and so a substantial number of the $^1\Pi$ levels lie between the two asymptotes. Excitation to these levels may then result in fragmentation along the $\text{Si}^+(^2P_{\frac{3}{2}}) + \text{H}(^2S)$ dissociation channel. We emphasize that the description of such levels as belonging to the $^1\Pi$ state is an approximation but it is a good starting point for the spectroscopic analysis.

The main features in the spectrum were obtained with the CR-590 broad-band laser and the complete spectrum from $15\,600$ to $18\,750 \text{ cm}^{-1}$ was then recorded with the CR-699-29 single-mode laser with a data-sampling interval of 75 MHz . Although this is a wider interval than the *fwhm* of the narrowest lines, it is sufficient to detect all but the weakest transitions. Each line was then examined in turn with a smaller sampling interval. A stick diagram of the spectrum is shown in figure 4 and the wavenumbers of the assigned lines are given in table 1. The quoted accuracy of each measurement varies according to the linewidth and intensity of the line.

The assignments could not have been achieved by using standard techniques such as combination differences etc., alone. The spectrum represents a small subset of all possible A–X transitions involving only those levels that lie just above the dissociation limit and with predissociation lifetimes lying approximately between $10 \mu\text{s}$ and 1 ps . These lifetime limits are set by the ion flight time in the apparatus and the breadth of the line respectively. Whereas molecular parameters for $v'' = 0, 1$ and 2 and $v' = 0, 1, 2$ and 3 are known from emission

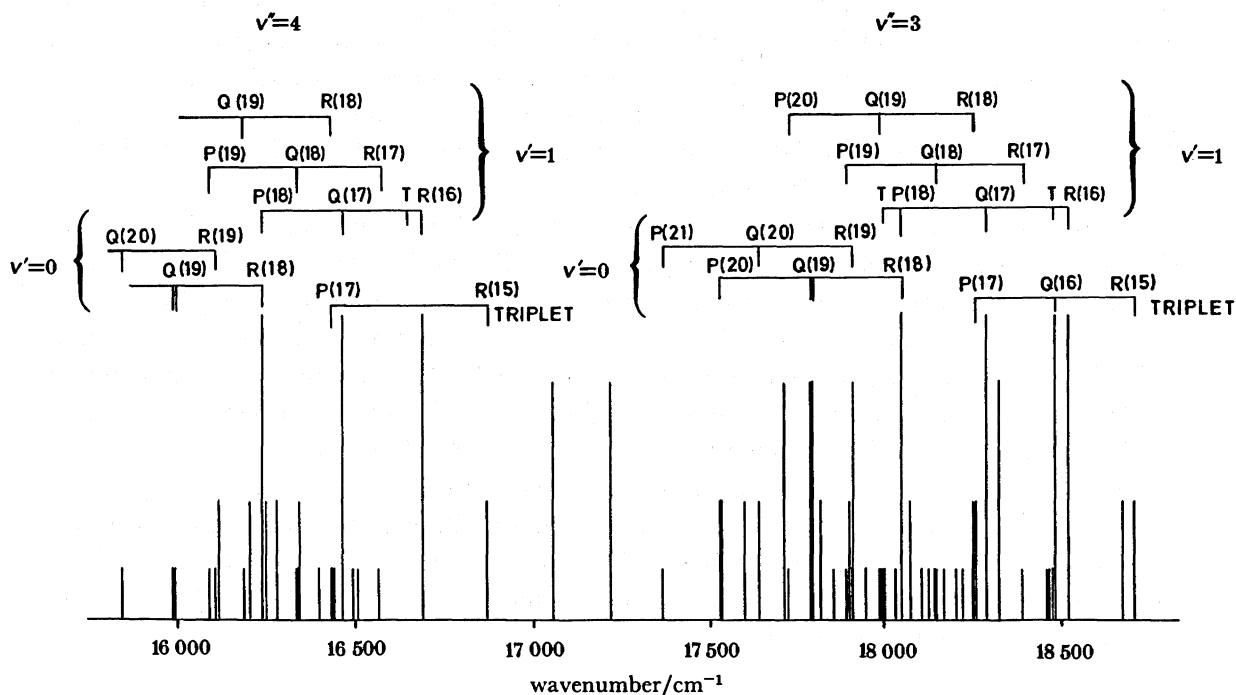


FIGURE 4. Stick diagram of the photofragment spectrum of SiH^+ obtained by the detection of Si^+ ions. The spectrum was recorded with a data sampling interval of 75 MHz at a scan rate of $5 \text{ cm}^{-1} \text{ min}^{-1}$ and with a 300 ms time constant. The experimental intensities are estimated values only.

TABLE 1. VACUUM WAVENUMBERS OF TRANSITIONS FROM THE $X^1\Sigma^+$ STATE TO EXCITED-STATE PREDISSOCIATED LEVELS (RESONANCES) OF SiH^+

(The transitions are to $A^1\Pi$ levels except for a number that have triplet (T) parentage.)

v'	v''	J'	R($J'-1$)	Q(J')	P($J'+1$)
0	3	19	18047.32 (1)†	17788.86 (1)	17526.56 (1)
	3	19 T‡	—	17795.51 (1)	—
0	4	19	16234.11 (1)	15983.29 (1)	—
	4	19 T	—	15989.94 (1)	—
0	3	20	17908.7 (1)	17638.60 (1)	17363.6 (1)
	4	20	16103.2 (1)	15841.06 (1)	—
	3	16 T	18701.51 (1)	18480.69 (1)	18255.73 (1)
	4	16 T	16867.79 (1)	—	16435.30 (1)
1	3	17	18518.91 (1)	18285.44 (1)	18047.85 (1)
	3	17 T	18472.84 (1)	—	18001.77 (1)
1	4	17	16691.64 (1)	16465.00 (1)	16234.65 (1)
	4	17 T	16645.57 (1)	—	—
1	3	18	18388.7 (1)	18145.2 (10)	17892.5 (1)
1	4	18	16568.3 (1)	16331.7 (10)	16087.0 (1)
1	3	19	18246.3 (10)	17989.4 (10)	17725.6 (10)
	4	19	16433.5 (10)	16183.5 (10)	—
2	3	18	—	18322.1 (2)	—
	4	18	—	16509.0 (10)	—

† The number in parentheses is the uncertainty in the last quoted figure(s).

‡ Levels labelled T have triplet parentage.

studies, the transitions are found to originate in $v'' = 3$ and 4, and an extrapolation to the levels of interest with Dunham coefficients is not possible. Fortunately, the laser-photofragment and energy-release spectra contain information that would not normally be obtained in an absorption spectrum and, coupled with a different theoretical approach, assignment of a substantial part of the spectrum has been achieved.

The spectrum of figure 4 shows that the lines are mostly clustered in regions near 18000 and 16000 cm^{-1} . The separation of these two regions is approximately the energy-level difference between $v'' = 4$ and $v'' = 3$ of the $X^1\Sigma^+$ state and so many of the lines in these two regions have common upper-state levels. Most of the lines carry a signature that is either a hyperfine splitting or a lifetime-broadened width as listed in table 2 and illustrated in figure 5. The measurement

TABLE 2. WIDTHS (RECIPROCAL CENTIMETRES) AND HYPERFINE SPLITTINGS (MEGAHERTZ) OF LINES OBSERVED IN THE VISIBLE LASER PHOTODISSOCIATION SPECTRUM OF SiH^+

v'	J'	e/f†	linewidth/ cm^{-1}	hyperfine splitting/MHz
0	19	e	< 0.0015	120 (10)
0	19	f	< 0.0015	—
	19	fT	< 0.0015	425 (10)
0	20	e	0.6 (1)‡	—
0	20	f	0.05 (1)	—
	16	eT	0.003 (1)	40 (20)
	16	fT	0.002 (1)	235 (10)
1	17	e	0.018 (3)	—
	17	eT	< 0.0015	270 (10)
1	17	f	0.002 (1)	150 (10)
1	18	e	0.5 (1)	—
1	18	f	3.0 (10)	—
1	19	e	2.5 (5)	—
1	19	f	4.5 (10)	—
2	18	f	4.5 (10)	—

† The e/f notation for the Λ -doublet components follows that given by Brown *et al.* (1975). The e and f levels are accessed in $\Delta J = \pm 1$ and $\Delta J = 0$ excitation respectively.

‡ The number in parentheses is the uncertainty in the last quoted figure(s).

of the energy released on fragmentation gives valuable information on the location of the energy level with respect to the dissociation channel, although the precision is very poor in comparison with the spectroscopic data. From the energy-release peak shape it is possible to determine if a transition involves $\Delta J = 0$ or $\Delta J = \pm 1$ excitation. For $\Delta J = 0$ (Q-line), the Si^+ fragments are ejected preferentially along the ion beam direction and this leads to a dip in the profile (see figure 6). For $\Delta J = \pm 1$ (R, P-lines), the scattering is perpendicular to the beam direction and a single peak results. The measured releases and profile information is given in table 3.

Following an approach used by Helm *et al.* (1982) in a study of shape resonances in CH^+ , the assignment of quantum numbers was achieved principally via numerical solution of the Schrödinger equation to calculate the energy levels in the two states. From the emission data (Carlson *et al.* 1980), numerical potentials have been derived for the lower parts of the $X^1\Sigma^+$ and $A^1\Pi$ states (M. Larsson, personal communication 1986). The long-range part of the

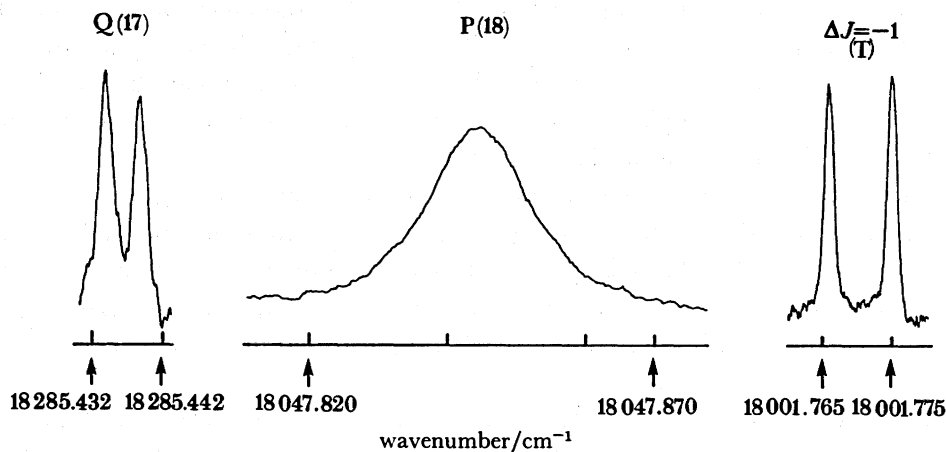


FIGURE 5. Spectroscopic transitions showing hyperfine structure and lifetime broadening for the Q (17) and P (18) lines of the 1-3 band and also for the corresponding $\Delta J = -1$ transition from $v'' = 3$, $J'' = 18$ to a triplet level (T) with $J' = 17$ (e). The hyperfine splitting in the Q (17) line is resolved only when the laser power is *ca.* 30 mW. The line involving the triplet level was recorded with a laser power of over 500 mW and does not exhibit power broadening.

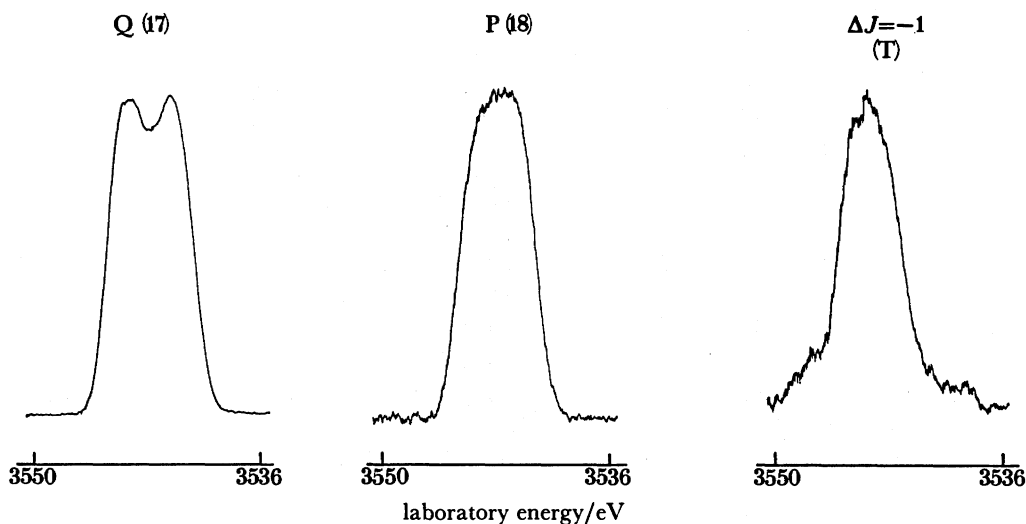


FIGURE 6. Energy-release profiles corresponding to laser excitation of the Q (17) and P (18) lines and to the triplet level of figure 5. The width of the energy release peak for excitation to the triplet $J' = 17$ level is narrower than for the P (18) line in agreement with the spectroscopic shift of -46.1 cm^{-1} (see figure 5 and table 2).

potentials were taken to be determined by the ion-induced dipole term $-C_4/R^4$, where C_4 is a constant involving the polarizability of the hydrogen atom. The two regions were linked smoothly with the shape forced to conform to the expression $-C_4/R^4 - C_6/R^6 - C_8/R^8$, where the C_6 and C_8 coefficients are free parameters. This is a crude approximation and other approaches are being evaluated. However, it is a particularly convenient form when a number of trial potentials with different dissociation energies are being explored. The short-range repulsive potential was linked smoothly using an exponential function. It is also necessary to define the dissociation energies of the states and recognize that the $^1\Sigma^+$ and $^1\Pi$ states correlate to different asymptotes (see figure 2). Initially, the published dissociation energies (Carlson *et al.* 1980)

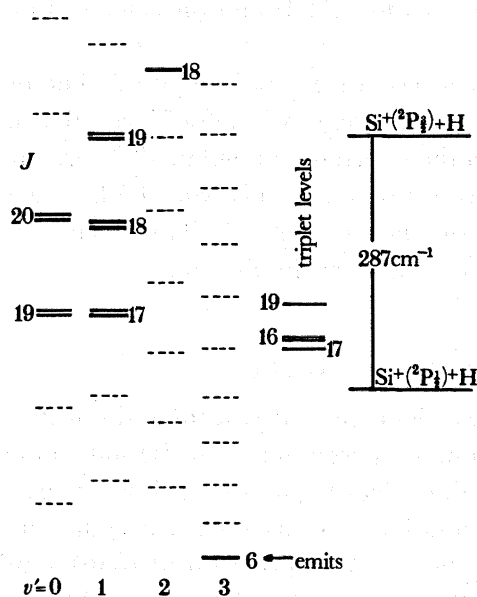


FIGURE 7. Identified singlet and triplet levels of SiH^+ close to the dissociation asymptotes. The Λ -doublet splittings are shown schematically and are not drawn to scale.

TABLE 3. CALCULATED AND EXPERIMENTAL 'ENERGY' RELEASES AND PEAK SHAPES ASSOCIATED WITH LASER EXCITATION TO THE RESONANCES LISTED IN TABLE 1

v'	J'	e/f	calculated/ $\text{cm}^{-1}\dagger$	experimental/ $\text{cm}^{-1}\ddagger$	peak shape§
0	19	e	92	102 (10)	S
0	19	f	92	—	—
	19	fT	99	—	—
0	20	e	203	202 (50)	—
0	20	f	203	—	—
	16	eT	54	55 (15)	S
	16	fT	54	72 (15)	D
1	17	e	92	95 (10)	S
1	17	f	92	107 (10)	D
	17	eT	46	49 (15)	S
1	18	e	191	187 (15)	S
1	18	f	191	215 (25)	—
1	19	e	290	312 (140)	—
2	18	f	363	395 (50)	—

\dagger Calculated level position with respect to the $^2\text{P}_1$ dissociation asymptote.

\ddagger 'Energy' release estimated from the FWHM of the peak.

\S S and D indicate that the peak shape is a single (S) or double (D) feature. Theoretically, the e and f levels should correspond to S and D, respectively (see text).

were employed but were later found to require upward revision. The bound and rotationally quasibound eigenvalues were determined by numerical solution of the Schrödinger equation for the chosen potentials by using a computer program of R. J. LeRoy (personal communication 1986). The effect of Λ -doubling in the $^1\Pi$ state is not included. We emphasize that these potentials are far from being spectroscopically accurate but this approach is much superior to the attempted extrapolation of molecular parameters to the levels of interest. The rotational line intensities were also calculated by using an *ab initio* electronic transition moment function

(M. Larsson, personal communication 1986) and the same computer program and also were of help in the assignment.

The near-threshold energy levels are shown in figure 7. The observation of emission from $v' = 3$, $J' = 6$ (Carlson *et al.* 1980), predissociation of levels that lie less than 287 cm^{-1} above this level and measurement of their corresponding kinetic-energy releases (table 3), necessarily means that most of the levels of interest in this work lie between the asymptotes as shown. It is important to establish this fact because the kinetic-energy releases do not carry any information on the fine-structure state of the Si^+ ion.

DISCUSSION

Tables 1 and 2 contain the assignments, linewidths and splittings. In many cases it has been possible to assign quantum numbers pertaining to the $^1\Pi$ state, but we also list other lines which involve excited-state levels with triplet (T) parentage. Transitions with $\Delta J = \pm 1$ (R, P) involve excitation to 'e' levels in the notation of Brown *et al.* (1975) that may be described alternatively as belonging to the 'A' parity block (Williams & Freed 1986). Similarly, the $\Delta J = 0$ (Q) lines involve the 'f' levels (in the 'B' parity block). The 'e' ('A') block contains levels from the $^1\Sigma^+$, $^1\Pi$, $^3\Pi_{2,1,0}$ and $^3\Sigma_1$ states and the 'f' ('B') block has levels from $^1\Pi$, $^3\Pi_{2,1,0}$ and $^3\Sigma_{1,0}$. For the near-threshold levels, the only strictly good quantum numbers are the total angular momentum, J , and parity (neglecting nuclear spin). Interactions between states can only occur with the selection rule $\Delta J = 0$ and within the same parity block. It follows that only one of the components of the $^1\Pi$ state is mixed with the ground state under the action of the Coriolis operator. This causes both the Λ -doublet splitting in the $^1\Pi$ state and also the Coriolis-induced predissociation of the 'e' component of the $^1\Pi$ state via the continuum of the ground electronic state.

The lines exhibit a very wide range of linewidths from the Doppler width of 0.0012 cm^{-1} to *ca.* 4.5 cm^{-1} . The variation in linewidths between 'e' and 'f' components and also with J value is indicative of erratic couplings of the levels and continua in the near-threshold region. Although it is attractive to attribute the greater linewidth of the 'e' relative to the 'f' component in the levels $v' = 0$, $J' = 20$ and $v' = 1$, $J' = 17$ to the effect of Coriolis coupling with the ground-state continuum, the reverse trend is found for $v' = 1$, $J' = 18$ and 19 , so it is clear that additional couplings with other states must be considered. In fact the Q-lines can only appear in the spectrum because of coupling with states of triplet parentage. Subject to the selection rules, all of the levels are subject to couplings with the shape resonances, Feshbach resonances and continua of the other singlet and triplet states in the vicinity. It is likely that a quantitative account for the predissociation linewidths will necessitate fully coupled multichannel calculations.

A consequence of non-adiabatic interactions is the appearance of the extra 'multichannel' resonances in the photodissociation spectrum as predicted theoretically (Singer *et al.* 1985; Williams & Freed 1986; Williams *et al.* 1987) and listed in tables 1–3. It is possible to assign the J and parity quantum numbers as indicated because of the spectroscopic line separations from identified singlet–singlet transitions or by extrapolation of ground-state level differences as in the case of the $J' = 16$ levels.

The narrow splittings in table 2 between 40 and 425 MHz are nuclear hyperfine splittings and arise from the presence of the proton nuclear spin of $\frac{1}{2}$. For a pure $^1\Pi$ state, only the

electronic orbital–nuclear hyperfine interaction is present but it will be of negligible magnitude for the high- J levels of interest here. For triplet levels or levels with triplet character, the Fermi contact (isotropic hyperfine coupling), spin–spin dipolar, orbital–nuclear and hyperfine-doubling interactions may contribute. The most important is expected to be the Fermi contact term, which provides a direct measure of the electron spin density at the proton nucleus. In the hydrogen atom, the Fermi contact parameter for an electron in the 1s orbital takes the value of 1420 MHz. However, for a molecule with a pure $^3\Pi$ state arising from a $\sigma^1\pi^1$ configuration, only half of the spin angular momentum contributes significantly to the spin density at the proton nucleus so the expected maximum observed splitting will be $1420/2 = 710$ MHz. All of the experimental splittings are indeed lower than this value. The existence of a splitting gives a qualitative indication of the triplet character in the wavefunction associated with a given resonance, although the absence of a splitting does not imply that the line involves a singlet level. Table 2 shows that even some of the levels which are nominally assigned to the $^1\Pi$ state can show significant splittings. The levels $v' = 0, J' = 19$ (e) and $v' = 1, J' = 17$ (f) exhibit splittings of 120 MHz and 150 MHz respectively because of the admixture of triplet character.

CONCLUSIONS

We have recorded and assigned a substantial part of the visible laser photodissociation spectrum of the SiH^+ ion and have established the principal features of the energy level (resonance) structure in the near-threshold region. The importance of non-adiabatic interactions is shown through the irregular behaviour of the linewidths, nuclear hyperfine splittings and the appearance of extra lines. Multichannel resonances are positively identified, we believe for the first time.

Ultimately, it is important to establish quantitative agreement between theory and the observed resonance energies, widths and hyperfine splittings. It seems improbable that a perturbation treatment will be able to achieve this objective and we are currently performing fully coupled calculations of the level (resonance) structure in an effort to achieve this objective.

We are most grateful to Dr D. M. Hirst for calculating the *ab initio* potential curves and for his interest in this work. We thank Professor R. J. LeRoy for a copy of the program LEVEL and Dr M. Larsson for sending the results of his work before publication. We have enjoyed many stimulating conversations with Professor K. F. Freed and Dr C. J. Williams.

We thank the SERC and the Research Corporation Trust for grants towards the purchase of apparatus and the SERC for a studentship to J.M.W.; P.J.S. thanks the Nuffield Foundation for the award of a Science Research Fellowship and C.J.W. thanks the National Westminster Bank for support of a University Research Studentship.

REFERENCES

- Berkowitz, J., Green, J. P., Cho, H. & Rušćić, B. 1987 *J. chem. Phys.* **86**, 1235–1248.
 Brown, J. M., Hougén, J. T., Huber, K.-P., Johns, J. W. C., Kopp, I., Lefebvre-Brion, H., Merer, A. J., Ramsay, D. A., Rostas, J. & Zare, R. N. 1975 *J. molec. Spectrosc.* **55**, 500–503.
 Bruna, P. J. & Peyerimhoff, S. D. 1983 *Bull. Soc. chim. Belg.* **92**, 525–546.
 Bruna, P. J., Hirsch, G., Bunker, R. J. & Peyerimhoff, S. D. 1983 In *Molecular ions – geometric and electronic structures* (ed. J. Berkowitz & K.-O. Groeneveld), p. 325. New York: Plenum.
 Carlson, T. A., Copley, J., Durić, N., Elander, N., Erman, P., Larsson, M. & Lyyra, M. 1980 *Astron. Astrophys.* **83**, 238–244.
 Carrington, A., Buttenshaw, J. A., Kennedy, R. A. & Softley, T. P. 1981 *Molec. Phys.* **44**, 1233–1237.

- Carrington, A., Kennedy, R. A., Softley, T. P., Fournier, P. G. & Richard, E. G. 1983 *Chem. Phys.* **81**, 251–261.
 Carrington, A. & Softley, T. P. 1985 *Chem. Phys.* **92**, 199–219.
 Carrington, A. & Softley, T. P. 1986 *Chem. Phys.* **106**, 315–338.
 Cosby, P. C., Helm, H. & Moseley, J. T. 1980 *Astrophys. J.* **235**, 52–56.
 Douglas, A. E. & Lutz, B. L. 1970 *Can. J. Phys.* **48**, 248–253.
 Graff, M. M., Moseley, J. T., Durup, J. & Roueff, E. 1983 *J. chem. Phys.* **78**, 2355–2362.
 Grevesse, N. & Sauval, A. J. 1970 *Astron. Astrophys.* **9**, 232–238.
 Helm, H., Cosby, P. C., Graff, M. M. & Moseley, J. T. 1982 *Phys. Rev. A* **25**, 304–321.
 Herzberg, G. & Mundie, L. G. 1940 *J. chem. Phys.* **8**, 263–273.
 Herzberg, G. 1950 In *Molecular structure and molecular spectra I, spectra of diatomic molecules*, p. 425. New York: van Nostrand.
 Hirst, D. M. 1986 *Chem. Phys. Lett.* **128**, 504–506.
 Hirst, D. M. 1987 *J. chem. Soc. Faraday Trans. II* **83**, 61–68.
 Hurley, A. C. 1961 *Proc. R. Soc. Lond. A* **261**, 237–245.
 Kaufman, S. L. 1976 *Optics Commun.* **17**, 309–312.
 Lefebvre-Brion, H. & Field, R. W. 1986 In *Perturbations in the spectra of diatomic molecules*. London: Academic Press.
 LeRoy, R. J. & Bernstein, R. H. 1970 *J. chem. Phys.* **52**, 3869–3879.
 Moseley, J. T. 1985 *Adv. chem. Phys.* **60**, 245–298.
 Sarre, P. J., Walmsley, J. M. & Whitham, C. J. 1986 *J. chem. Soc. Faraday Trans. II* **82**, 1243–1255.
 Sarre, P. J., Walmsley, J. M. & Whitham, C. J. 1987 *Faraday Discuss. chem. Soc.* **82**, 67–78.
 Sarre, P. J. & Whitham, C. J. 1987 (In preparation.)
 Singer, S. J., Freed, K. F. & Band, Y. B. 1985 *Adv. chem. Phys.* **61**, 1–113.
 Stwalley, W. C. 1978 *Contemp. Phys.* **19**, 65–80.
 Williams, C. J. & Freed, K. F. 1986 *J. chem. Phys.* **85**, 2699–2717 and *Chem. Phys. Lett.* **127**, 360–366.
 Williams, C. J., Freed, K. F., Singer, S. J. & Band, Y. B. 1987 *Faraday Discuss. chem. Soc.* **82**, 51–66.

Discussion

G. DUXBURY (*Department of Physics and Applied Physics, University of Strathclyde, Glasgow, U.K.*)
 Dr Sarre and his group have carried out some elegant experiments to show the many resonances that can occur when highly excited states of the diatomic ions SiH^+ and CH^+ interact with continuum states.

In their work on the polyatomic ions, SiH_2^+ and PH_2^+ more complex behaviour is observed. Much of the $\tilde{A}^2B_1-\tilde{X}^2A_1$ spectrum of SiH_2^+ can be understood within the framework of Renner–Teller coupling (Curtis *et al.* 1985). However, in part of the SiH_2^+ spectrum and in the spectrum of PH_2^+ detected via P^+ or PH^+ the explanation is not as clear cut (Jackson 1985). One possible explanation of the spectra involves an extension of the system of diatomic resonance to the polyatomic case, the other is outlined below.

Some recent experiments by Reutt *et al.* (1986) shed some light on possible processes occurring. They carried out molecular-beam photoelectron spectroscopy of both H_2O^+ and D_2O^+ , and have interpreted their results as from two principal causes, Renner–Teller coupling between the \tilde{A}^2A_1 and \tilde{X}^2B_1 states, and curve crossing between the \tilde{B}^2B_2 and \tilde{A}^2A_1 states. This interpretation is based on an autocorrelation function analysis of the high-resolution photoelectron spectra of cold H_2O^+ and D_2O^+ . Even though the levels of the 2B_2 state are very highly excited, the possibility of multiple intersection between potential-energy surfaces, particularly the conical intersection between the 2B_2 and 2A_1 surface, is held to be the principal route to rapid decay of the excited state, rather than coupling to the continuum. The possibilities of a much wider range of surface crossings in polyatomic species make the classification of interaction with the continuum states much more complicated than in diatomic molecules.

References

- Curtis, M. C., Jackson, P. A., Sarre, P. J. & Whitham, C. J. 1985 *Molec. Phys.* **56**, 485–488.
 Jackson, P. A. 1985 Ph.D. thesis, University of Nottingham, U.K.
 Reutt, J. E., Wang, L. S., Lee, Y. T. & Shirley, D. A. 1986 *J. chem. Phys.* **85**, 6928–6939.